Adsorption, desorption, and diffusion of *k*-mers on a one-dimensional lattice

I. Lončarević and Lj. Budinski-Petković
Faculty of Engineering, Trg D. Obradovića 6, Novi Sad 21000, Serbia

S. B. Vrhovac* and A. Belić
Institute of Physics, P.O. Box 68, Zemun, 11080 Belgrade, Serbia

(Received 28 March 2009; published 20 August 2009)

Kinetics of the deposition process of *k*-mers in the presence of desorption or/and diffusional relaxation of particles is studied by Monte Carlo method on a one-dimensional lattice. For reversible deposition of *k*-mers, we find that after the initial "jamming," a stretched exponential growth of the coverage $\theta(t)$ toward the steady-state value θ_{eq} occurs, i.e., $\theta_{eq}-\theta(t)\propto\exp[-(t/\tau)^{\beta}]$. The characteristic time scale τ is found to decrease with desorption probability P_{des} according to a power law, $\tau\propto P_{des}^{-\gamma}$, with the same exponent $\gamma=1.22\pm0.04$ for all *k*-mers. For irreversible deposition with diffusional relaxation, the growth of the coverage $\theta(t)$ above the jamming limit to the closest packing limit (CPL) θ_{CPL} is described by the pattern $\theta_{\mathrm{CPL}}-\theta(t)\propto E_{\beta}[-(t/\tau)^{\beta}]$, where E_{β} denotes the Mittag-Leffler function of order $\beta\in(0,1)$. Similarly to the reversible case, we found that the dependence of the relaxation time τ on the diffusion probability P_{dif} is consistent again with a simple power-law, i.e., $\tau\propto P_{dif}^{-\delta}$. When adsorption, desorption, and diffusion occur simultaneously, coverage always reaches an equilibrium value θ_{eq}, which depends only on the desorption/adsorption probability ratio. The presence of diffusion only hastens the approach to the equilibrium state, so that the stretched exponential function gives a very accurate description of the deposition kinetics of these processes in the whole range above the jamming limit.

DOI: 10.1103/PhysRevE.80.021115 PACS number(s): 02.50.−r, 68.43.Mn, 68.43.Nr, 05.10.Ln

I. INTRODUCTION

The process of random sequential adsorption (RSA) models a large variety of physical, chemical, and biological processes where events occur essentially irreversibly, and where equilibration due to spatial diffusion is slow compared to the time scales of interest [1–3]. Learning about the mechanisms and kinetics of these phenomena is of a fundamental importance in a large field of applications which include the deposition of colloidal particles, polymer chains and proteins on a surface [4–7].

In the RSA model, particles are added randomly and sequentially onto a substrate without overlapping each other. RSA model assumes that deposited particles can neither diffuse along, nor desorb from the surface. The kinetic properties of a deposition process are described by the time evolution of the coverage $\theta(t)$, which is the fraction of the substrate area covered by the adsorbed particles. Within a monolayer deposit, each adsorbed particle affects the geometry of all later placements. Due to the blocking of the substrate area by the already randomly adsorbed particles, at large times the coverage approaches the jammed-state value θ_{jam}, where only gaps too small to fit new particles are left in the monolayer. The resulting state is less dense than the fully ordered close packed coverage.

Depending on the system of interest, the substrate can be continuum or discrete. Asymptotic approach of the coverage fraction $\theta(t)$ to its jamming limit $\theta_{jam}=\theta(t\to\infty)$ is known to be given by an algebraic time dependence for continuum systems [8–12]. For lattice RSA models the approach to the jamming coverage is exponential [13–18],

$$\theta(t)=\theta_{jam}-Ae^{-t/\sigma}, \tag{1.1}$$

where A and σ are parameters that depend on the details of the model, such as shape and orientational freedom of depositing objects.

However, in many real physical situations it is necessary to consider the possibility of desorption or diffusion of deposited particles [19–22]. Allowing desorption makes the process reversible and the system ultimately reaches an equilibrium state. The density of particles in the steady state is a function only of the desorption to adsorption rate ratio [23,24]. Approach of the coverage to its equilibrium value was found to be exponential for the adsorption-desorption processes on a line [23]. However, a power-law time dependence of the coverage followed by an exponential relaxation to equilibrium was suggested for the reversible RSA of *k*-mers on a one-dimensional (1D) lattice [25]. Results of the numerical simulations of reversible RSA on a triangular lattice obtained for a wide variety of object shapes [26] showed an excellent agreement of the relaxation dynamics with the Mittag-Leffler function which is a natural generalization of the exponential function. Much attention has been paid to the adsorption-desorption processes on continuum substrates, but there are very few studies concerning the adsorption-desorption processes even on one-dimensional lattices.

Adsorption processes with diffusional relaxation are widely studied [27–29] because of their relevance to various systems where diffusional rearrangement of deposited particles is observable on the time scales of the deposition process. At very early times of the process, when the coverage is small, the adsorption process is dominant. With the growth of the coverage, diffusion becomes more important and at the late times additional adsorption events are possible only on

*slobodan.vrhovac@scl.rs; http://www.phy.bg.ac.rs/~vrhovac/

the holes formed by the diffusion of the adsorbed objects. On a one-dimensional lattice RSA with diffusional relaxation finally leads to a fully covered lattice. In two dimensions such processes lead to formation of large clusters of covered sites. After long enough times only few frozen defects, whose dimensions are less than the dimensions of the depositing objects, remain unoccupied [30]. For irreversible deposition with diffusional relaxation most of the authors propose a power-law time dependence of the coverage at the late stages of deposition [27–29].

Despite of the relative simplicity of one-dimensional problems, there are no exact results for adsorption-desorption processes, nor for irreversible deposition with diffusional relaxation on the 1D lattice. Here we present the results of extensive numerical simulations of the reversible RSA and of the deposition with diffusional relaxation of k-mers on the 1D lattice. We also study the case where all three processes, adsorption, desorption, and diffusion, are present simultaneously. We focus our attention on the intermediate- to long-time behavior of the coverage fraction $\theta(t)$. In particular, we try to find a universal functional type that describes the growth of the coverage $\theta(t)$ in the whole range above the jamming limit θ_{jam} in the best way.

The paper is organized as follows. Section II describes the details of the simulations. Approach of the coverage fraction $\theta(t)$ to the equilibrium coverage in the case of adsorption-desorption processes is discussed in Sec. III. Results of the simulations of the adsorption processes with diffusional relaxation are analyzed in Sec. IV, and the results for the case where all three processes—adsorption, desorption, and diffusion are present simultaneously are given in Sec. V. Finally, Sec. VI contains some additional comments and final remarks.

II. SIMULATION METHOD

The Monte Carlo simulations of adsorption-desorption processes, adsorption processes with diffusional relaxation and processes where adsorption, desorption, and diffusion are present simultaneously are performed on a one-dimensional lattice of size $L=10^5$ with a periodic boundary condition. The adsorbing objects are k-mers covering $k=2$, 4, 6, 8, and 10 sites. Adsorption, desorption and diffusion attempts are statistically independent and they perform sequentially with corresponding probabilities. The time t is counted by the number of adsorption attempts and scaled by the total number of lattice sites L. The data are averaged over 100 independent runs for each of the investigated processes and for each choice of k-mer.

At each Monte Carlo step adsorption is attempted with probability P_a and desorption with probability P_{des}. In the case of adsorption-desorption processes the kinetics is governed by the ratio of desorption to adsorption probability P_{des}/P_a [20,26]. Since we are interested in the ratio P_{des}/P_a, in order to save computer time, it is convenient to take the adsorption probability to be $P_a=1$. For each of these processes a lattice site is selected at random. In the case of adsorption, we try to place the k-mer with the beginning at the selected site, i.e., we search whether k consecutive sites in a randomly chosen direction are unoccupied. If so, we place the object. Otherwise, we reject the deposition trial. When the attempted process is desorption, and if a beginning of a deposited k-mer is at the selected site, the object is removed from the layer.

In the simulations of adsorption processes with diffusional relaxation only the ratio of diffusion to adsorption probability is relevant. At each Monte Carlo step adsorption is tried with probability $P_a=1$ and diffusion with probability P_{dif}. In the case of adsorption a lattice site is selected at random and deposition of a k-mer with the beginning at the selected site is tried. When the attempted process is diffusion and if there is a beginning of the deposited object at the randomly selected site, we choose one of the two possible directions at random and try to move the selected k-mer for a lattice constant in that direction. The object is moved if it does not overlap with any of the deposited objects. On the contrary, the attempt is abandoned.

When adsorption, desorption, and diffusion perform simultaneously, the kinetics of the process is determined by the ratios of both desorption/adsorption and diffusion/adsorption probabilities [31]. At each Monte Carlo step adsorption is attempted with probability $P_a=1$, desorption with probability P_{des} and diffusion with probability P_{dif}. For each of these processes a lattice site is selected at random. In the case of adsorption, we try to place the k-mer with the beginning at the selected site. When the attempted process is desorption, and provided that the selected site is a beginning of a deposited k-mer, the object is removed from the layer. If the attempted process is diffusion, and if there is a beginning of a previously deposited object at the randomly selected site, we choose one of the two possible directions at random and try to move the k-mer for a lattice constant in that direction.

III. ADSORPTION-DESORPTION PROCESSES ON A ONE-DIMENSIONAL LATTICE

Adsorption-desorption processes on one-dimensional substrates display a surprisingly complex kinetics [21,25]. Here we consider the case of rapid adsorption and slow desorption ($P_{des}/P_a \ll 1$). Then there exist two time scales controlling the evolution of the coverage $\theta(t)$. The first stage of the process is dominated by adsorption events and the kinetics displays an RSA-like behavior. With the growth of the coverage the desorption process becomes more and more important. Increasing the coverage over the jamming limit is possible only due to the collective rearrangement of the adsorbed particles in order to open a hole large enough for the adsorption of an additional particle. We are interested in the approach to the equilibrium coverage in this later, post-jamming time range.

Simulations of the adsorption-desorption processes of k-mers were performed for a wide range of desorption probabilities and for all $k \leq 10$. On the basis of these results we have examined different functional forms looking for a function that gives the best fit to our simulation results. We find that the stretched exponential relaxation of the form

$$\theta(t) = \theta_{eq} - \Delta\theta \exp[-(t/\tau)^{\beta}] \tag{3.1}$$

describes the approach to the equilibrium state in a very precise manner. The values of the equilibrium coverage θ_{eq}, the

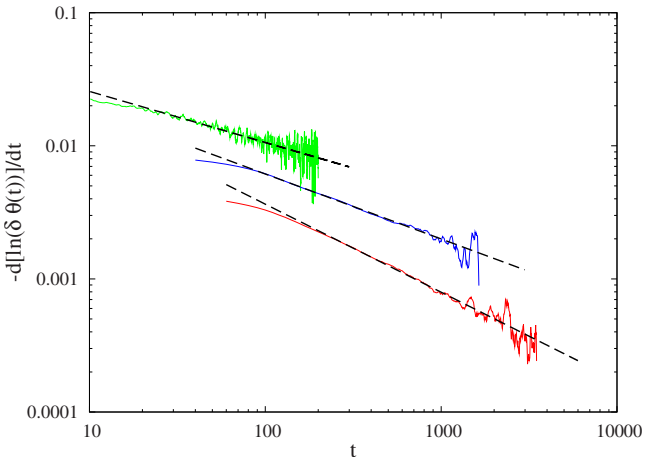

FIG. 1. (Color online) Test for the presence of the stretched exponential law [Eq. (3.1)] in the time dependence of coverage $\theta(t)$ for $k=2$ (red, bottom curve), $k=4$ (blue, middle curve), and $k=8$ (green, upper curve). Straight line sections of the curves show where the law holds. The dashed lines are power-law fits of Eq. (3.5). All the results are for $P_{des}=0.005$.

parameter $\Delta\theta$ and the relaxation time τ depend on the length of the k-mer and on the desorption probability.

In order to gain an additional confirmation of the stretched exponential behavior in the case of adsorption-desorption processes, we can make the analysis that follows. Function (3.1) can be written as

$$\delta\theta(t) = \Delta\theta \exp(-(t/\tau)^{\beta}), \tag{3.2}$$

where $\delta\theta = \theta_{eq} - \theta(t)$. Differentiation of Eq. (3.2) gives

$$\frac{d\delta\theta(t)}{dt} = -\Delta\theta \exp(-(t/\tau)^{\beta}) \frac{\beta}{\tau}\left(\frac{t}{\tau}\right)^{\beta-1}, \tag{3.3}$$

i.e.,

$$-\frac{1}{\delta\theta(t)}\frac{d\delta\theta(t)}{dt} = \frac{\beta}{\tau^{\beta}} t^{\beta-1}. \tag{3.4}$$

From Eq. (3.4) it follows

$$-\frac{d}{dt}\{\ln[\delta\theta(t)]\} = \frac{\beta}{\tau^{\beta}} t^{\beta-1}, \tag{3.5}$$

which means that a double logarithmic plot of the derivative of $\ln[\delta\theta(t)]$ vs t is a straight line in the case of the stretched exponential function (3.1).

The derivatives of $\ln[\delta\theta(t)]$ are calculated numerically for the data obtained by Monte Carlo simulations of adsorption-desorption processes. The double logarithmic plots of $-d\{\ln[\delta\theta(t)]\}/dt$ are straight lines for all the k-mers and for all values of desorption probabilities. Representative examples of such plots are shown in Fig. 1 for $k=2$, 4, 8 and $P_{des}=0.005$. This suggests that the relaxation to the equilibrium state in the case of adsorption-desorption processes on the one-dimensional lattice is well described by the stretched exponential function of the form (3.1). Values of the fitting parameters β and τ are determined from the slopes of these

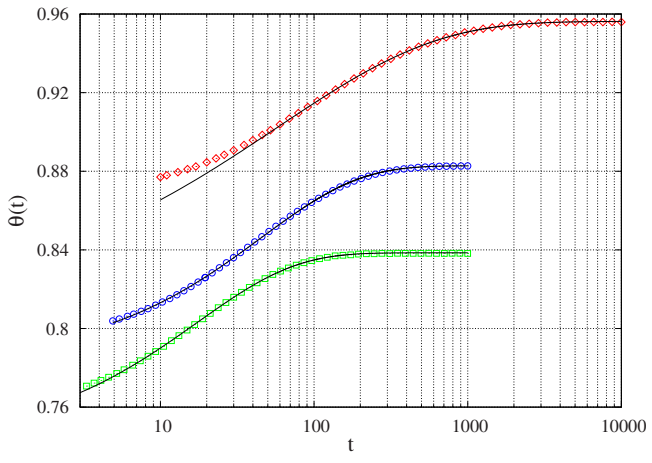

FIG. 2. (Color online) Temporal behavior of the coverage $\theta(t)$ for $k=2$ (◇), $k=4$ (○), and $k=8$ (□) in the case of reversible RSA. The continuous curves are the stretched exponential fits of Eq. (3.1), with the parameters τ and β given in Figs. 4 and 5, respectively. All the results are for $P_{des}=0.01$.

lines. The fitting values of the parameter $\Delta\theta$ are obtained for each pair (τ,β) by using the least-squares method.

In Figs. 2 and 3 results of the numerical simulations are shown together with the stretched exponential fitting functions where the corresponding parameters τ, β, and $\Delta\theta$ are obtained as described above. The plots of the simulation data and the corresponding stretched exponential functions are given in Fig. 2 for three different k-mers for $P_{des}=0.01$ and in Fig. 3 for three different desorption probabilities for $k=6$. We can see that the stretched exponential fitting function shows an excellent agreement with the simulation results in the region above the jamming coverage.

Dependence of τ on the desorption probability is shown on a double logarithmic scale in Fig. 4. For all the k-mers these plots are straight lines approximately parallel to each other, indicating that the relaxation time τ is a simple power-law of the desorption probability

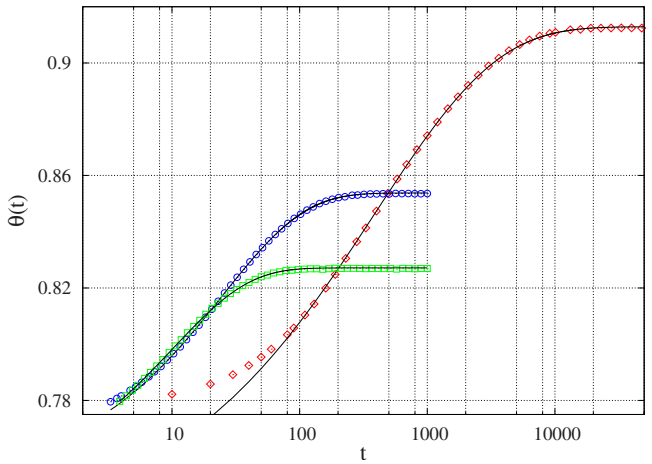

FIG. 3. (Color online) Temporal behavior of the coverage $\theta(t)$ for $P_{des}=0.001$ (◇), $P_{des}=0.01$ (○), and $P_{des}=0.02$ (□). The continuous curves are the stretched exponential fits of Eq. (3.1), with the parameters τ and β given in Figs. 4 and 5, respectively. All the results are for $k=6$.

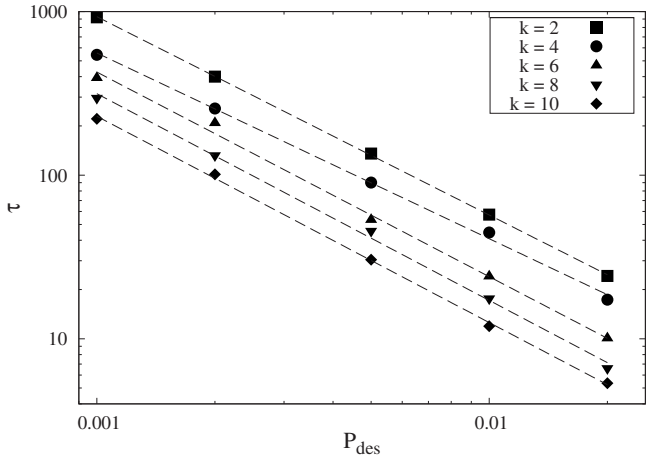

FIG. 4. Parameter τ of the stretched exponential fit [Eq. (3.1)] vs desorption probability P_{des} for the cases of $k=2,4,6,8,10$. The dashed lines are the power-law fits of Eq. (3.6), with the same exponent $\gamma=1.22\pm0.04$ for all the k-mers.

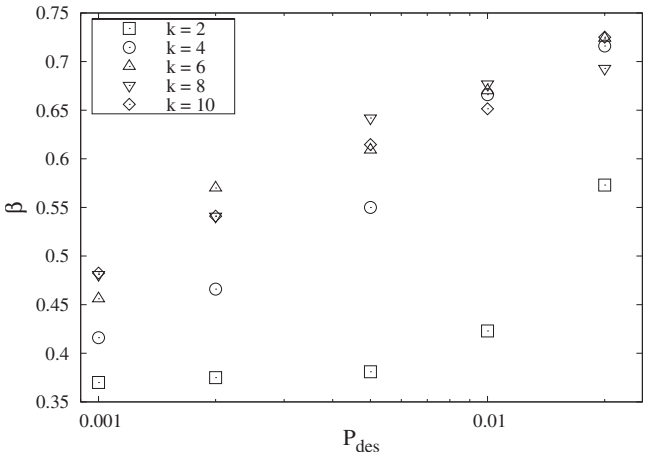

FIG. 5. Parameter β of the stretched exponential fit [Eq. (3.1)] vs desorption probability P_{des} for the cases of $k=2,4,6,8,10$.

$$\tau = AP_{des}^{-\gamma}, \tag{3.6}$$

with the same exponent $\gamma=1.22\pm0.04$ for all k-mers. The parameter A depends on the length of the k-mer.

As seen in Figs. 2 and 4, the shorter k-mers have larger values of the relaxation time τ. This means that the deposition dynamics gets drastically slower when k decreases, especially for low values of P_{des}. A qualitative interpretation of these results can be attained by exploiting the mechanism of collective events for governing the late-time changes in the coverage fraction. In the initial stages of the process, desorption events are negligible compared to adsorption. When a value of θ_{jam} is reached, the rare desorption events are generally followed by immediate readsorption. The total number of particles is not changed by these *single*-particle events. However, when one badly sited object desorbs and two particles adsorb in the opened good locations, then the number of particles is increased by one. On the contrary, if two well sited objects desorb and a single object adsorbs in their stead, the number of particles is decreased by one. These *collective* events are responsible for the density growth above θ_{jam} [20,32]. The length of the k-mers have a crucial influence on the filling of small isolated targets on the lattice that are left for deposition in the late times of the process. Indeed, for the shorter k-mer there is a greater number of possible isolated locations for deposition and an enhanced probability for readsorption. Hence, the decrease of the length of the k-mer enhances the rate of *single*-particle readsorption. This extends the mean waiting time between consecutive two-particle events responsible for the coverage growth and causes a slowing down of the densification.

Dependence of the fitting parameter β on the desorption probability is shown in Fig. 5 for $k=2,4,6,8,10$. We can see that the stretching exponent β depends on the ratio P_{des}/P_a. For small values of P_{des}/P_a the coverage fraction does not significantly change near the jamming limit θ_{jam} and the evolution takes place on a much wider time scale. In other words, the smaller are the values of P_{des}/P_a, the longer the system remains around the jamming limit. This dynamical behavior is characterized by the small values of the stretching exponent β and can be associated with the competition of single and multiparticle events. Indeed, the single-particle events are capable of bringing the system to its jamming limit θ_{jam} in a given time t. If t was small enough compared to the two-particle transition rate, the system would stay at $\theta(t)\gtrapprox\theta_{jam}$ until the two-particle events contributed to the dynamics. This results in the plateau in the time evolution of the coverage fraction near the jamming limit. This is illustrated in Fig. 3, which shows the ending of plateau in coverage $\theta(t)$ just above the jamming limit $\theta_{jam}=0.7794$ for $P_{des}=0.001$. The length of this plateau is controlled by the ratio P_{des}/P_a and the object size, as these quantities determine the transition rates both for two "well-placed" particles to one "not well-placed" particle and one not well-placed particle to two well-placed particles [20,25]. It is obvious that this relaxation behavior disappears in the regime of strong desorption, $P_{des}\to1$, when the stretching exponent $\beta\to1$.

IV. RSA WITH DIFFUSIONAL RELAXATION

In this section we report the numerical studies of the effects of diffusion on RSA in 1D. Looking for a function that gives the best fit to the coverage fraction $\theta(t)$ in the case of irreversible deposition with diffusional relaxation, we have tried the wide set of phenomenological fitting functions for relaxation processes in many complex disordered systems [33]. The best agreement with our simulation data was obtained by the Mittag-Leffler function. The fitting function we have used is of the form

$$\theta(t) = \theta_{\mathrm{CPL}} - \Delta\theta E_{\beta}[-(t/\tau)^{\beta}], \tag{4.1}$$

where θ_{CPL}, $\Delta\theta$, τ, and β are the fitting parameters. Parameter τ determines the characteristic time of the coverage evolution and β measures the rate of deposition process on this time scale. When the deposited k-mers are subject to diffusion, the coverage fraction approaches the closest packing

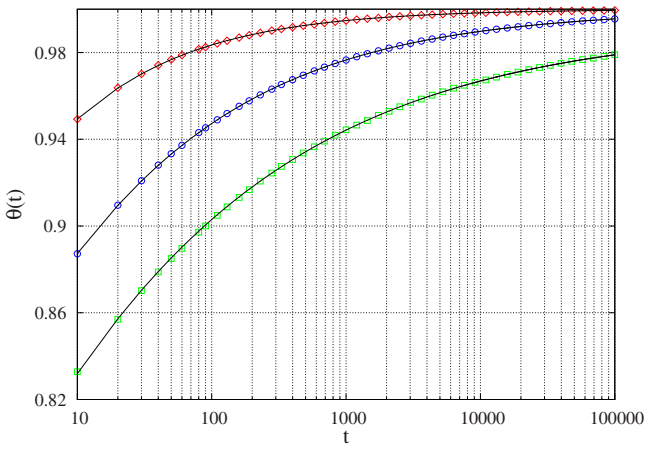

FIG. 6. (Color online) Temporal behavior of the coverage $\theta(t)$ for $k=2$ ($\diamond$), $k=4$ ($\bigcirc$), and $k=8$ ($\square$) in the case of irreversible deposition with diffusional relaxation. The continuous curves are the Mittag-Leffler fits of Eq. (4.1). All the results are for $P_{dif}=0.7$.

limit θ_{CPL} for large times, $t\to\infty$; in the case of 1D lattice, $\theta_{\mathrm{CPL}}=1$ [27,29]. In Eq. (4.1), E_β denotes the Mittag-Leffler function of order β [34]. It is defined through the inverse Laplace transform $\mathcal{L}$

$$E_\beta[-(t/\tau)^\beta] = \mathcal{L}[(u+\tau^{-\beta}u^{1-\beta})^{-1}], \tag{4.2}$$

from which the series expansion

$$E_\beta[-(t/\tau)^\beta] = \sum_{n=0}^{\infty} \frac{[-(t/\tau)^\beta]^n}{\Gamma(1+\beta n)}, \tag{4.3}$$

can be deduced; in particular, $E_1(-t/\tau)=\exp(-t/\tau)$. The Mittag-Leffler function interpolates between the initial stretched exponential form

$$E_\beta[-(t/\tau)^\beta] \sim \exp\left[-\frac{1}{\Gamma(1+\beta)}(t/\tau)^\beta\right], \quad t \ll \tau, \tag{4.4}$$

and the long-time power-law behavior

$$E_\beta[-(t/\tau)^\beta] \sim \frac{1}{\Gamma(1-\beta)}(t/\tau)^{-\beta}, \quad t \gg \tau. \tag{4.5}$$

Using Eqs. (4.1), (4.4), and (4.5) one obtains that the time dependence of the coverage behaves as

$$\theta(t) \sim \theta_{\mathrm{CPL}} - \Delta\theta \exp\left[-\frac{1}{\Gamma(1+\beta)}(t/\tau)^\beta\right], \quad t \ll \tau, \tag{4.6}$$

and

$$\theta(t) \sim \theta_{\mathrm{CPL}} - \Delta\theta \frac{1}{\Gamma(1-\beta)}(t/\tau)^{-\beta}, \quad t \gg \tau. \tag{4.7}$$

The Mittag-Leffler fits of the coverage fraction $\theta(t)$ are shown in Fig. 6 for three different k-mers ($k=2,4,8$) and for $P_{dif}=0.7$. Furthermore, in Fig. 7 we also present the fits to Eq. (4.1) in the case of 4-mers for three values of

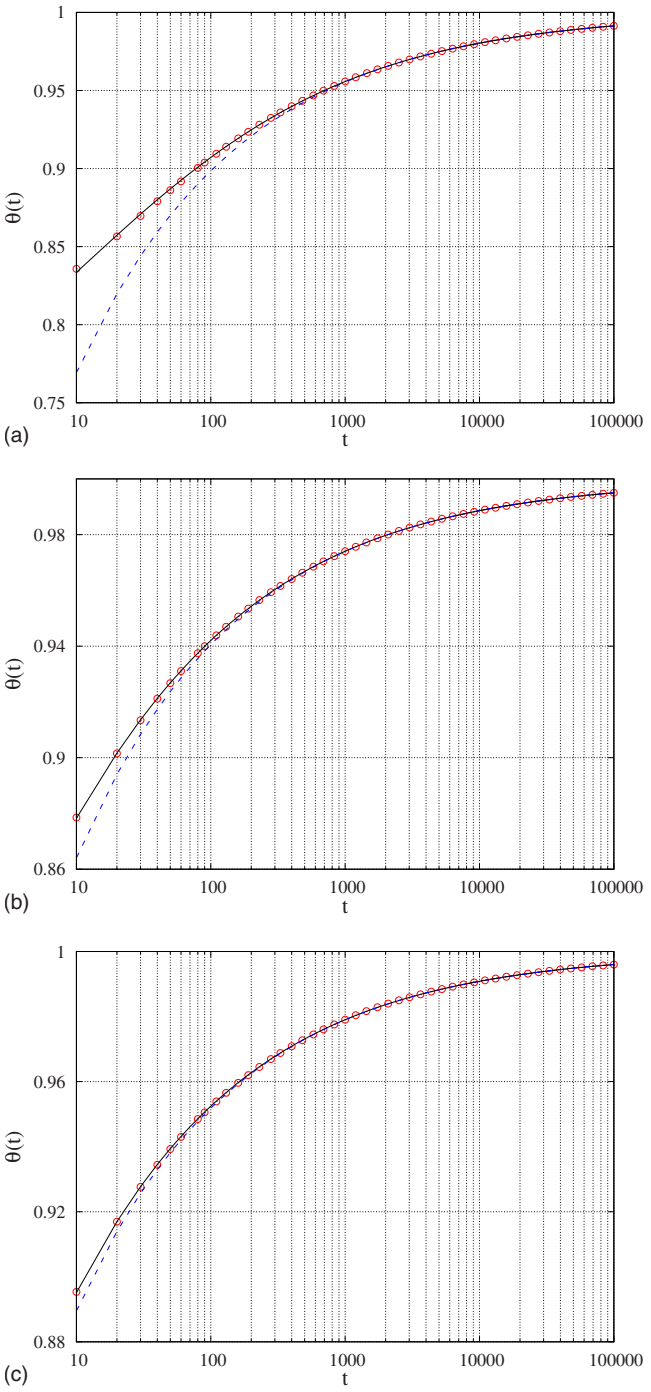

FIG. 7. (Color online) Temporal behavior of the coverage $\theta(t)$ (circles) for $k=4$ and for: (a) $P_{dif}=0.1$, (b) $P_{dif}=0.5$, and (c) $P_{dif}=1.0$. The continuous curves are the Mittag-Leffler fits of Eq. (4.1), and the dashed curves are the power-law fits of Eq. (4.8).

$P_{dif}=0.1,0.5,1.0$. We can see that the Mittag-Leffler function gives an excellent agreement with the simulation data forcoverages above the θ_{jam}. Also included in Fig. 7 are the comparisons of the Mittag-Leffler fits [Eq. (4.1)] and the power-law fits of the form

$$\theta(t) = \theta_{\mathrm{CPL}} - \Delta\theta t^{-\beta}, \tag{4.8}$$

where $\Delta\theta$ and β denote the fitting parameters that depend on the length of k-mer and on the diffusion probability P_{dif}. As

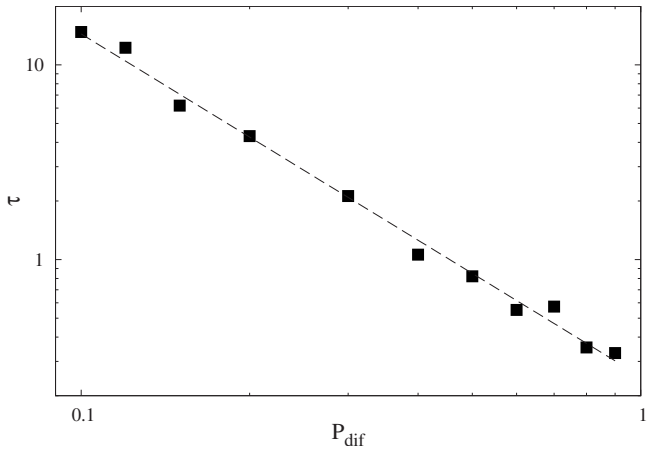

FIG. 8. Parameter τ of the Mittag-Leffler fit (4.1) vs diffusion probability P_{dif} for $k=4$. The dashed curve is the power-law fit of Eq. (4.9), with $\delta=1.76\pm0.03$ and $A=0.25\pm0.01$.

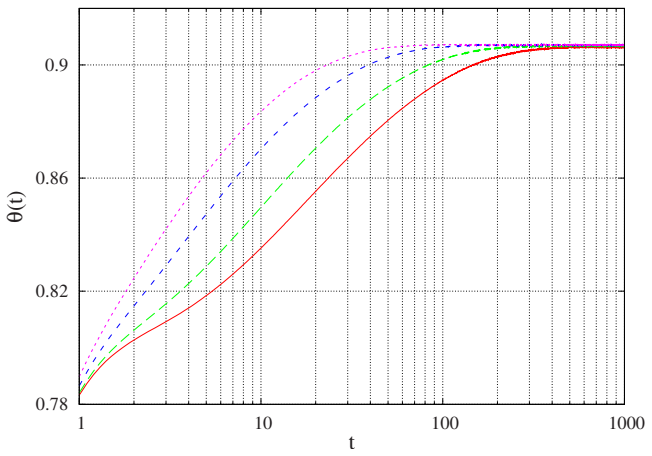

FIG. 9. (Color online) Temporal behavior of the coverage $\theta(t)$ for $k=4$ and for $P_{dif}=0.1$ (red, solid), $P_{dif}=0.2$ (green, long dashed), $P_{dif}=0.5$ (blue, short dashed), and $P_{dif}=1.0$ (violet, dotted). All the results are for $P_{des}=0.005$.

it can be seen, at the late times of the deposition process the coverage fraction $\theta(t)$ approaches the closest packing limit according to a power law [Eq. (4.8)] which is in agreement with the previous results [27–29]. In 1D, the power-law behavior is related to the coverage growth at large times by the process of hopping and recombination of small empty regions [27]. The values for parameter β obtained by least-square fits of the coverage $\theta(t)$ for large t are roughly consistent with the mean-field relation $1-\theta(t\text{-}\text{“large”})\propto t^{1/(k-1)}$ for $k\geq3$ [27,35]. Our simulation results for β exceed the mean-field values about 6% in the whole range of diffusion probability P_{dif} considered. For the deposition of dimers ($k=2$) we find that the closest packing limit $\theta_{\mathrm{CPL}}=1$ is approached according to the $\sim1/\sqrt{t}$ power-law [27,35].

It is obvious that the Mittag-Leffler fit [Eq. (4.1)] precisely describes the adsorption process with diffusional relaxation on a wider time scale than the power law [Eq. (4.8)]. It must be stressed that the Mittag-Leffler pattern [Eq. (4.1)] is consistent with the power-law behavior for large times. Indeed, according to [Eq. (4.7)] the Mittag-Leffler function behaves as the power-law function for the late times of the process.

A double logarithmic plot of the relaxation time τ vs the diffusion probability P_{dif} shown in Fig. 8 for $k=4$ suggests a simple power-law dependence of τ on P_{dif},

$$\tau=AP_{dif}^{-\delta}. \tag{4.9}$$

Similar plots are obtained for all k-mers, but with different slopes. The values of the parameter δ obtained from these slopes are $\delta=1.46\pm0.02$, 1.76 ± 0.03, 3.13 ± 0.03, 3.64 ± 0.04, and 3.58 ± 0.05 for $k=2$, 4, 6, 8, and 10, respectively.

V. ADSORPTION-DESORPTION PROCESSES WITH DIFFUSIONAL RELAXATION

Here we consider the general case of reversible RSA of k-mers on 1D lattice in the presence of diffusion. The simulations are performed for a wide range of desorption and diffusion probabilities. When adsorption, desorption, and diffusion perform simultaneously, system always reaches an equilibrium state. The equilibrium coverage θ_{eq} depends only on the desorption/adsorption probability ratio [31,36] and the presence of diffusion only hastens the approach to the equilibrium state. This is illustrated in Fig. 9 where the time dependence of the coverage $\theta(t)$ in the case of reversible deposition of 4-mers is shown for various values of diffusion probabilities, $P_{dif}=0.1$, 0.2, 0.5, and 1.0. As can be seen at coverages above θ_{jam}, the rearrangement of the k-mers on the lattice is more rapid and the equilibrium is reached more quickly for greater diffusion probabilities.

We could say that the nature of the time behavior of the coverage in the adsorption-desorption processes with diffusional relaxation is predominantly determined by the presence of desorption. The system always reaches a steady state in which the adsorption flux is exactly balanced by the desorption flux. The stretched exponential function, used as the fitting function for the adsorption-desorption processes [Eq. (3.1)], gives a very accurate description of the deposition kinetics of these processes. The values of the fitting parameters β and τ are obtained using the double logarithmic plots of derivatives of $\ln(\delta\theta(t))$, as in the case of the adsorption-desorption processes [see Eq. (3.5)]. Results of the simulations and the corresponding fitting functions are given in Fig. 10 for three different combinations of desorption and diffusion probabilities.

Dependence of the relaxation time τ on the diffusion probability is shown in Fig. 11 for a few fixed desorption probabilities in the case of 4-mers. Similar dependence is obtained for other k-mers. The linear fits through the data points suggest that in the presence of desorption the relaxation time shows a simple power-law dependence on the diffusion probability, of the same form (4.9) as in the case of irreversible deposition with diffusional relaxation. For fixed diffusion probabilities τ decreases with desorption probability as shown in Fig. 12 for $k=4$.

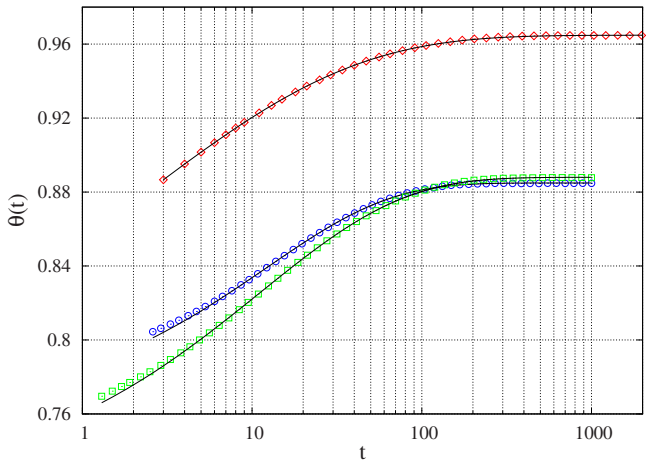

FIG. 10. (Color online) Temporal behavior of the coverage $\theta(t)$ for $k=2$ ($\diamond$), $k=4$ ($\bigcirc$), and $k=8$ ($\square$) in the case of reversible RSA with diffusional relaxation. The continuous curves are the stretched exponential fits of Eq. (3.1). The simulation parameters (P_{des}, P_{dif}) are (0.005, 0.2), (0.01, 0.1), and (0.002, 0.5) for $k=2,4,8$, respectively.

VI. CONCLUSIONS

We have investigated numerically the kinetics of deposition process of k-mers on a 1D lattice in the presence of desorption or/and diffusion of particles. We focused on the time evolution of the coverage $\theta(t)$ in the whole postjamming time range $(\theta(t) > \theta_{jam})$. In order to obtain the best agreement with our simulation data, a systematic approach was made by examining a wide variety of phenomenological fitting functions as candidates for slow relaxation processes in our system.

First, it was shown that the stretched exponential behavior [Eq. (3.1)] excellently describes the coverage dynamics above the jamming limit in the case of reversible deposition of k-mers. We have also pointed out the importance of multiparticle transitions for governing the late-time behavior of the coverage.

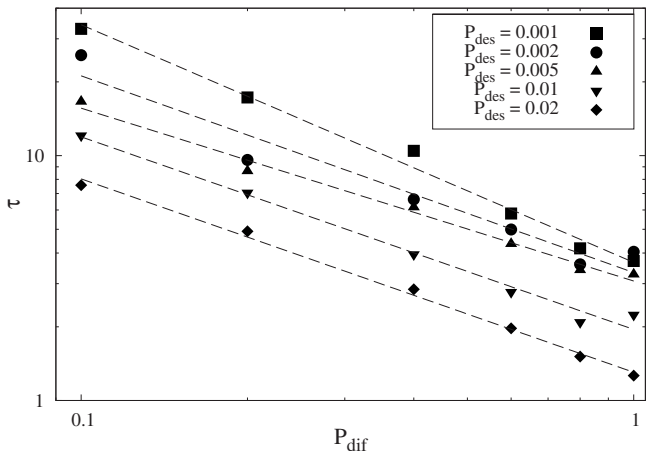

FIG. 11. Parameter τ of the stretched exponential fit [Eq. (3.1)] vs diffusion probability P_{dif} for the cases of P_{des} $=0.001,0.002,0.005,0.01,0.02$. The dashed lines are the power-law fits of Eq. (4.9), with exponent $\gamma \in (0.7-1.0)$. All the results are for $k=4$.

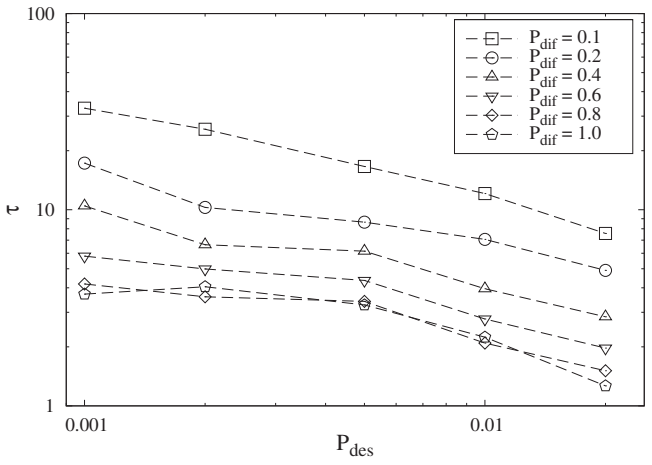

FIG. 12. Parameter τ of the stretched exponential fit [Eq. (3.1)] vs desorption probability P_{des} for the cases of P_{dif} $=0.1,0.2,0.4,0.6,0.8,1.0$. All the results are for $k=4$. The dashed lines are a guide to the eyes.

The adsorption-desorption model is frequently used by many authors to reproduce qualitatively the densification kinetics and other features of weakly vibrated granular materials [21,22,37]. The model describes the density relaxation of a given slice of a granular material, perpendicular to the tapping force. As a result of a tapping event, particles leave the layer at random (desorption events). Compaction proceeds when particles fall back into the layer under the influence of gravity (adsorption events). The ratio of desorption to adsorption probability, P_{des}/P_a, within the model plays a role similar to that of the intensity of vibration in real experiments. Note that the dynamics of the reversible RSA model depends on the excluded volume and geometrical frustration, just as in the case of granular compaction. Different laws have been proposed for increasing packing fraction of a granular material with the number of taps [38]. More recently, Bideau and co-workers [39,40] have found experimentally that the compaction dynamics is consistent with the stretched exponential law [Eq. (3.1)]. Hence, we have directly confirmed that the reversible RSA model on a 1D lattice describes the slow relaxation and dynamics of compaction in real granular systems in an excellent way.

We found that when diffusion is introduced in RSA processes, the growth of the coverage $\theta(t)$ above the jamming limit θ_{jam} to the closest packing limit $\theta_{\mathrm{CPL}} \approx 1$ occurs via the Mittag-Leffler law [Eq. (4.1)], for all values of k and all diffusion probabilities P_{dif}. The characteristic time scale τ is found to decrease with the diffusion probability P_{dif} according to a power law [Eq. (4.9)], $\tau \propto P_{dif}^{-\delta}$. This kind of power-law scaling was also observed in the stretched exponential fits [Eq. (3.1)] of the coverage fraction in lattice based reversible RSA model (Sec. III). We have shown that the parameter τ in this model decreases algebraically with desorption probability P_{des}, as in Eq. (3.6).

In any realistic systems, adsorption, desorption, and diffusional relaxations should all occur simultaneously with nonzero probabilities. In that case, our results indicate the

same postjamming kinetics as for $P_{dif}=0$ [see, Eq. (3.1)]. The possibility of diffusion of the objects hastens the evolution of the coverage toward the steady-state value θ_{eq} that depends only on the desorption/adsorption probability ratio. In the presence of diffusion, equilibrium is always reached for shorter time than in the case of a pure adsorption-desorption process.

ACKNOWLEDGMENTS

This work was supported by the Ministry of Science of the Republic of Serbia, under Grant No. 141035. The simulations were performed in the Center for Meteorology and Environmental prediction—Advanced Computing Laboratory.

[1] J. W. Evans, Rev. Mod. Phys. **65**, 1281 (1993).
[2] V. Privman, Colloids Surf., A **165**, 231 (2000).
[3] A. Cadilhe, N. A. M. Araújo, and V. Privman, J. Phys.: Condens. Matter **19**, 065124 (2007).
[4] P. J. Flory, J. Am. Chem. Soc. **61**, 1518 (1939).
[5] J. J. Ramsden, Phys. Rev. Lett. **71**, 295 (1993).
[6] J. Talbot, G. Tarjus, P. R. Van Tassel, and P. Viot, Colloids Surf., A **165**, 287 (2000).
[7] B. Senger, J. C. Voegel, and P. Schaaf, Colloids Surf., A **165**, 255 (2000).
[8] J. Feder, J. Theor. Biol. **87**, 237 (1980).
[9] R. H. Swendsen, Phys. Rev. A **24**, 504 (1981).
[10] Y. Pomeau, J. Phys. A **13**, L193 (1980).
[11] B. Bonnier, Phys. Rev. E **64**, 066111 (2001).
[12] D. J. Burridge and Y. Mao, Phys. Rev. E **69**, 037102 (2004).
[13] M. C. Bartelt and V. Privman, J. Chem. Phys. **93**, 6820 (1990).
[14] P. Nielaba, V. Privman, and J. S. Wang, J. Phys. A **23**, L1187 (1990).
[15] S. S. Manna and N. M. Švrakić, J. Phys. A **24**, L671 (1991).
[16] Lj. Budinski-Petković and U. Kozmidis-Luburić, Phys. Rev. E **56**, 6904 (1997).
[17] Lj. Budinski-Petković and U. Kozmidis-Luburić, Physica A **236**, 211 (1997).
[18] Lj. Budinski-Petković, S. B. Vrhovac, and I. Lončarević, Phys. Rev. E **78**, 061603 (2008).
[19] J. J. Ramsden, G. I. Bachmanova, and A. I. Archakov, Phys. Rev. E **50**, 5072 (1994).
[20] R. S. Ghaskadvi and M. Dennin, Phys. Rev. E **61**, 1232 (2000).
[21] J. Talbot, G. Tarjus, and P. Viot, Phys. Rev. E **61**, 5429 (2000).
[22] Lj. Budinski-Petković and S. B. Vrhovac, Eur. Phys. J. E **16**, 89 (2005).
[23] P. L. Krapivsky and E. Ben-Naim, J. Chem. Phys. **100**, 6778 (1994).
[24] Lj. Budinski-Petković and U. Kozmidis-Luburić, Physica A **301**, 174 (2001).
[25] P. Ranjith and J. F. Marko, Phys. Rev. E **74**, 041602 (2006).
[26] Lj. Budinski-Petković, M. Petković, Z. M. Jakšić, and S. B. Vrhovac, Phys. Rev. E **72**, 046118 (2005).
[27] V. Privman and P. Nielaba, Europhys. Lett. **18**, 673 (1992).
[28] C. Fusco, P. Gallo, A. Petri, and M. Rovere, J. Chem. Phys. **114**, 7563 (2001).
[29] J. W. Lee and B. H. Hong, J. Chem. Phys. **119**, 533 (2003).
[30] J.-S. Wang, P. Nielaba, and V. Privman, Physica A **199**, 527 (1993).
[31] Lj. Budinski-Petković and T. Tošić, Physica A **329**, 350 (2003).
[32] A. J. Kolan, E. R. Nowak, and A. V. Tkachenko, Phys. Rev. E **59**, 3094 (1999).
[33] R. Hilfer, J. Non-Cryst. Solids **305**, 122 (2002).
[34] E. W. Weisstein, *Mittag-leffler function*, From MathWorld–A Wolfram Web Resource, http://mathworld.wolfram.com/Mittag-LefflerFunction.html
[35] V. Privman and M. Barma, J. Chem. Phys. **97**, 6714 (1992).
[36] J. R. G. de Mendonca and M. J. de Oliveira, J. Stat. Phys. **92**, 651 (1998).
[37] G. Tarjus and P. Viot, Phys. Rev. E **69**, 011307 (2004).
[38] G. Lumay and N. Vandewalle, Phys. Rev. E **74**, 021301 (2006).
[39] P. Philippe and D. Bideau, Europhys. Lett. **60**, 677 (2002).
[40] P. Ribière, P. Richard, D. Bideau, and R. Delannay, Eur. Phys. J. E **16**, 415 (2005).